Optimal shepherding and transport of a flock

Aditya Ranganathan,[1] Alexander Heyde,[2] Anupam Gupta,[3] and L. Mahadevan[1, 2, 4]

[1]*Paulson School of Engineering and Applied Sciences, Harvard University, Cambridge, MA 02138*
[2]*Department of Organismic & Evolutionary Biology, Harvard University, Cambridge, MA 02138*
[3]*Department of Physics, Indian Institute of Technology, Hyderabad 502284*
[4]*Department of Physics, Harvard University, Cambridge, MA 02138*

We investigate how a shepherd should move in order to effectively herd and guide a flock of agents towards a target. Using a detailed agent-based model (ABM) for the members of the flock, we pose and solve an optimization problem for the shepherd that has to simultaneously work to keep the flock cohesive while coercing it towards a prescribed project. We find that three distinct strategies emerge as potential solutions as a function of just two parameters: the ratio of herd size to shepherd repulsion length and the ratio of herd speed to shepherd speed. We term these as: (i) mustering, in which the shepherd circles the herd to ensure compactness, (ii) droving, in which the shepherd chases the herd in a desired direction, and (iii) driving, a hitherto unreported strategy where the flock surrounds a shepherd that drives it from within. A minimal dynamical model for the size, shape and position of the herd captures the effective behavior of the ABM, and further allows us to characterize the different herding strategies in terms of the behavior of the shepherd that librates (mustering), oscillates (droving) or moves steadily (driving). All together, our study yields a simple and intuitive classification of herding strategies that ought to be of general interest in the context of controlling the collective behavior of active matter.

The complex patterns by which social organisms establish and maintain flocking behavior have long fascinated scientists [1–4]. Herds must exhibit several key characteristics, including species recognition, spatial awareness, and orientational alignment in order to achieve successful organized movement [1, 5]. This concert of coordinated cognition often occurs in the presence of a nearby threat or predator—for example, sheep flocking in response to a shepherding dog; indeed Hamilton's selfish herd theory proposes that this flocking occurs due to the simultaneous effort on the part of each individual to minimize its own predation risk by moving towards a group's center [6]. This individual-level mechanism may explain empirical observations that the approach of a shepherding dog prompts a strong attraction towards the center of the herd [7]. However, although Hamilton's theory addresses why a herd may form and compress, it does not explain the emergence of orientational alignment and organized movement of the herd, both of which are exploited by a shepherd to guide the herd towards a target location.

Both in the animal behavior community and in the physical modeling community, the self-organized aspects of herding have garnered much attention and work. One class of particularly impactful flocking models [2, 4, 8–12] focus on constructing dynamical rules for the interaction of agents based on attraction, alignment, and repulsion, including the foundational swarming model of Vicsek et al. [1] and its fruitful elaboration, e.g. [2, 3]. Far fewer have attempted to model the evasive response of a herd to a nearby threat or predator [13, 14], and fewer still have studied how a shepherd exploits this response to guide a herd [15, 16]. In contrast there have been many applications of shepherding in crowd management [17, 18], en-

vironmental cleanup [19], livestock herding [20, 21], and swarm robotics [22]. Common to these real-world examples of shepherding is a pattern of first aggregating individuals into a group, and second, transporting the group in a desired direction.

In this paper, we explore the question of how to move a herd from one location to another using a shepherd that interacts repulsively with an otherwise cohesive flock. We build on the attraction, alignment, and repulsion models prevalent in the collective behavior literature to explore the emergence of optimal herding strategies. While there are different metrics with respect to which optimality may be defined, we focus our attention on the metrics of herd aggregation and transport. In contrast to previous studies on herding algorithms [15, 16], our approach does not specify any algorithms for shepherding at the outset. Instead, we show that the real-world patterns of herding behavior are emergent, being the consequence of both the shepherd trying to optimize the movement of the herd towards a target at every timestep as well as the interaction rules obeyed by agents in the herd. The advantage of such an approach is that no specific conditions for shepherd behavior need to be specified at the outset of a herding process; the behavior is entirely dependent on the sampling and optimization of an objective function over time, and as such can evolve and adapt different classes of behavior.

We first begin by developing a minimal shepherding model that results in distinct patterns of transport, each pattern emerging as the optimal solution in different regions of phase-space corresponding to different sizes of herds, as well as different speeds of shepherds (dogs, humans, drones, etc). We first develop the model as a

microscopic agent-based model (ABM) formulation and then proceed to reframe the model in the (very coarse-grained) ODE limit to show that the essential features of the model can be captured in both the agent-based and ODE models. Together, the models present complementary frameworks for the investigation of optimal transport and navigation in herding. We show that our ABM model leads to the emergence of three strategies of shepherding as a function of the herd size (relative to the shepherd repulsion scale), and the speed of the shepherd (relative to that of the agents in the flock), consistent with the results of the ODE model. Finally, a minimal dynamical picture in terms of the motion of the shepherd allows us to provide an intuitive picture of the different shepherding modalities and the relative efficiencies of the strategies.

Agent-based model

In its simplest formulation, our model studies a population of N self-propelled agents moving in a two-dimensional open field, where they interact with each other and a nearby shepherd. Our minimal model of agent-agent interactions reframes the work of Reynolds, Vicsek, and Couzin [1, 2, 8] and captures the following features of real-world flocks: first, directed motion of the entire flock, second, the nonzero area occupied by each agent, and third, the safety that agents find within a herd (as compared with an isolated agent). Any model of shepherding must also include an interaction (assumed to be repulsive) between the shepherd and the agents being herded. Combining these four interactions yields the following generalized form for the velocity field of a given agent in the herd, with α, β, γ, δ representing weights for each term:

$$\boldsymbol{v}^{\text{net}} = \alpha\boldsymbol{v}_{a-a}^{\text{alignment}} + \beta\boldsymbol{v}_{a-a}^{\text{repulsion}} + \gamma\boldsymbol{v}_{a-a}^{\text{attraction}} + \delta\boldsymbol{v}_{a-s}^{\text{repulsion}}, \tag{1}$$

,
where three agent-agent interactions are local alignment ($\boldsymbol{v}_{a-a}^{\text{alignment}}$), finite agent size ($\boldsymbol{v}_{a-a}^{\text{repulsion}}$), and weak attraction to the herd center ($\boldsymbol{v}_{a-a}^{\text{attraction}}$); and the shepherd-agent interaction is given by $\boldsymbol{v}_{a-s}^{\text{repulsion}}$.

The first term on the RHS of [1] states that agents close to each other align their velocity vectors, giving rise to coordinated herd motion and breaking of rotational symmetry [1]. This term also dictates the inherent speed at which agents move, v_a, in a shepherd-free world. Our model implements alignment using the same formulation as the Vicsek model [1] with

$$\boldsymbol{v}_{a-a}^{\text{alignment}}(i) = v_a\hat{\boldsymbol{v}}^{\text{alignment}}(i), \tag{2}$$

where $\hat{\boldsymbol{v}}^{\text{alignment}}(i) =$

$(\cos\theta^{\text{alignment}}(i), \sin\theta^{\text{alignment}}(i))$ is the local preferred velocity orientation of the i-th agent as a function of the average orientation of its neighbors. Each agent's orientation is updated continuously to be the average orientation $\langle\theta\rangle$ of neighbors within an interaction radius $r^{\text{alignment}}$, taken to be $\sim 10l_a$ with a uniformly distributed additive noise $\eta \in [-\eta_0/2, \eta_0/2]$, such that the update for the polar alignment angle of the i-th agent, $\theta^{\text{alignment}}(i)$, is given by

$$\theta^{\text{alignment}}(i) = \langle\theta\rangle_{r<r^{\text{alignment}}} + \eta. \tag{3}$$

The second term in [1[states that flocks may not collapse into a single point. The finite size of agents is modeled in our framework as an exponential repulsion between agents at length scales, $\sim l_a$, which also sets the characteristic agent size in the model. Thus, the i-th agent experiences a repulsion due to all the other agents of the form

$$\boldsymbol{v}_{a-a}^{\text{repulsion}}(i) = \sum_{i \neq j} \exp(-r_{ji}/l_a)\hat{\boldsymbol{r}}_{ji}, \tag{4}$$

where $\boldsymbol{r}_{ji} = \boldsymbol{r}_i - \boldsymbol{r}_j$, $\boldsymbol{r}_i = (x_i, y_i)$ represents the position vector of the i-th agent, the $\hat{}$ symbol denotes the unit vector, and the magnitude of a vector $\boldsymbol{p}$ is represented by p.

The third term in [1] quantifies the idea of the selfish herd [6]; agents in wild flocks and herds avoid detection and capture by predators [7] by feeling a feel a pull towards the center of the herd $\boldsymbol{r}_{\text{cm}}$. As seen in videos of sheep and other herds, the long-range attraction commonly manifests itself as the convergence of two sub-herds into a larger cohesive whole. The speed of convergence seems to match the default agent speed v_a regardless of the distance of any particular agent from the center of mass of the herd. Consequently, we implement an attraction term of constant magnitude everywhere. The velocity contribution takes the form

$$\text{v}_{a-a}^{\text{attraction}}(i) = v_a\left(\cos\phi(i), \sin\phi(i)\right), \tag{5}$$

where

$$\phi(i) = \tan^{-1}\left(\frac{y_{\text{cm}} - y_i}{x_{\text{cm}} - x_i}\right)$$

represents the polar angle between the agent and the center of mass of the herd as shown in Fig 1.

The final interaction in [1] is based on predator-prey dynamics observed in nature; when pursued by a shepherd (perceived as a 'predator') moving at a speed v_s, members of a herd experience a repulsion away from the shepherd located at $\boldsymbol{r}_s$. This repulsion is clearly dependent on the distance between the shepherd, which brings
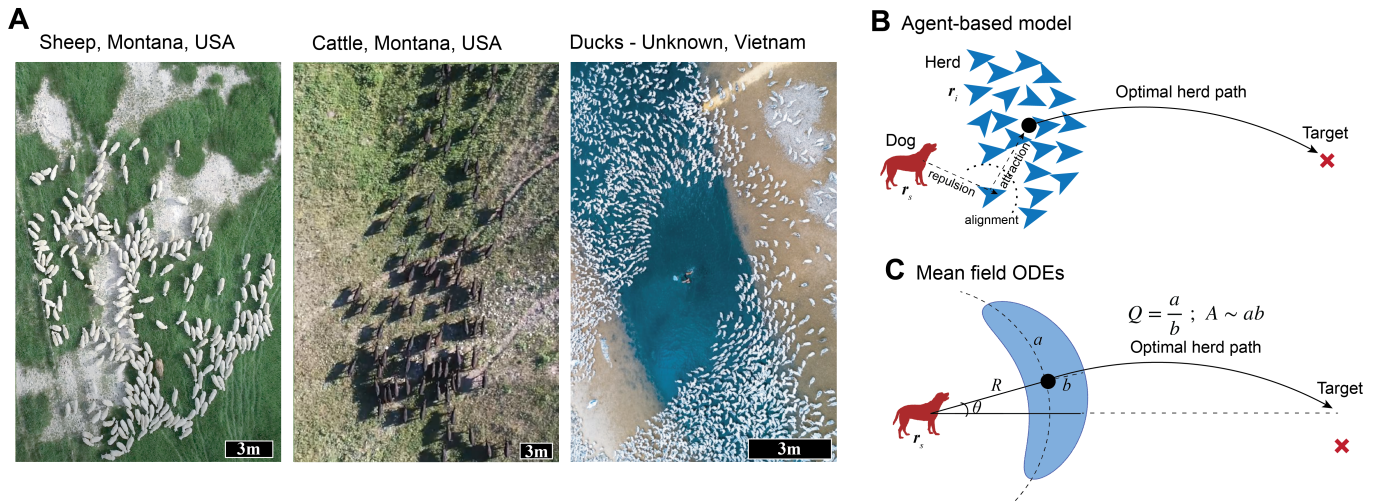
FIG. 1: Model schematic across three formulations. (A) Real world images of herding in action for different species. From left to right, shows a tightly bound herd, a moving herd with alignment between agents, and a herd clustered around the shepherd who is encased within the herd. (B) In our agent-based formulation, the position and orientation of individual herd members (blue arrows) respond to each other and the location of a nearby dog (red) that moves so as to optimally transport the herd center (black dot) to the target location (red cross). (C) In our mean-field ODE formulation, the herd is modeled as an ellipse in polar space with area A and aspect ratio Q that evolve in response to the distance R to the dog. Sheep and Cattle images courtesy of Jordan Kennedy (© Jordan Kennedy, 2022) Ducks image by Wai Soen, viewable on Pinterest (https://www.pinterest.com.mx/pin/gallery-skypixels-jawdropping-drone-photos-of-the-year–49469295890894303/).

in a natural length scale over which the repulsion between the shepherd and an agent will decay, l_s. In our simulations, we chose $l_s \sim 30 l_a$ which yields all phases of herding behavior (Fig. 4) and was initially based on observations of real-world shepherds in which a single shepherd can often control herds between 10-100 agents. For the i-th agent, this looks like

$$\boldsymbol{v}_{a-s}^{\text{repulsion}}(i) = \exp(-r_{si}/l_s)\hat{\boldsymbol{r}}_{si}, \qquad (6)$$

where $\boldsymbol{r}_{si} = \boldsymbol{r}_i - \boldsymbol{r}_s$.

Having now constructed a model of the herd's response to agents within the herd and to an external shepherd, we now turn our attention to the dynamics of the shepherd. We assume that the goal of the shepherd is to take advantage of the agents' self-organization and as a result, transport the herd more effectively than it could transport the individual agents themselves, one at a time. The movement of the shepherd over time $\boldsymbol{r}_s(t)$ determines the control input in our model, leading to the question: what is the optimal shepherding movement or strategy?

In order for a transport to be effective, the shepherd must transport all agents from an initial point to a final point. This broad goal naturally leads to three specific conditions: (A) the shepherd should attempt to move the center of mass of the herd to the desired location; (B) the shepherd may not lose agents in the process. A transport is only successful if every agent is transported. This requirement places an emphasis on maintaining herd

cohesion. If a herd splinters or splits, the shepherd has not achieved success. (C) the shepherd should keep both the target and herd in alignment, as much as possible so as to maintain line of sight and minimize extraneous diversions in the transport path. Given that each of these conditions can be viewed as competing pulls on the shepherd's behavior, we define an objective function for the shepherd as a linear combination of the transport requirements with weights W_{mean}, W_{std}, and W_{col} corresponding to condition (A), (B), and (C) respectively, which we write as

$$C(\boldsymbol{r}_s; \boldsymbol{r}_{\text{target}}, \boldsymbol{r}_a) = W_{\text{mean}}|\Delta r| + W_{\text{std}}\sigma_{r_{cm}} + W_{\text{col}}\Delta|R_{col}|, \qquad (7)$$

where the first term $|\Delta r| = |\boldsymbol{r}_{\text{target}} - \boldsymbol{r}_{\text{cm}}|$ represents the importance of transporting the herd to the target, the second term $\sigma_{r_{\text{cm}}} = \left[\frac{\sum_i (r_i - r_{\text{cm}})^4}{N}\right]^{\frac{1}{4}}$ represents the importance of cohesion, and the third term $\Delta\boldsymbol{R}_{col} = \boldsymbol{r}_s + l_s\hat{\boldsymbol{r}}_{\text{cm}-\text{target}}$ represents the the advantage gained from keeping the entire flock within the line of sight of the shepherd (situational awareness), where $\boldsymbol{r}_{\text{cm}-\text{target}}$ represents the vector from the center of mass of the herd to the target. The emphasis or weights that a shepherd must place on the different conditions depends on the behavior of the agents in the herd; for example, if the attraction between agents is high (large γ in equation 1) then the shepherd need not emphasize herd cohesion ($W_{\text{std}} \to 0$).

In order to explore optimal behavior, the agent-based model was simulated using a home brewed forward Euler scheme in C++. The behavior of the shepherd was determined by a discrete gradient descent approach at each timestep (corresponding to a 'decision point' in the trajectory). At each step, several randomly selected directions, chosen from a uniform distribution between $[0, 2\pi)$ were tested and the direction corresponding to the minimal objective function value was chosen by the shepherd. Classification of shepherd behavior into the different emergent strategies or phases was done upon completion of the simulation using a python script.

Parameters for simulations were chosen to resemble real-world phenomena where possible. For example, based on evidence that herding dogs in the wild can control 10-100 sheep, we chose the number of agents in the simulations to initially be $N \sim 50$ [7]. The speed ratio of the shepherd to the agents $\frac{v_s}{v_a}$ was controlled by setting the agents' grazing speed to a constant and varying v_s which can be viewed as the shepherds 'hunting' speed. Neither v_a nor v_s should be viewed as the true top speed of agents or shepherds in the wild. While simulations explored several orders of magnitude of the speed ratios, most simulations that show resemblance to real-world examples of hunting fall into a narrower window of speed ranges (see Fig. 4).

The weights for the objective function were chosen on the assumption that losing agents in a herd was most unacceptable. Alignment was least important. As a result, the standard weights used in the objective function were: $W_{\mathrm{mean}}/W_{\mathrm{std}} \sim 0.1$, and $W_{\mathrm{col}}/W_{\mathrm{std}} \sim 0.001$.

The phase space of optimal shepherd behavior (Fig. 4) was explored using a custom built bash script to launch $\sim 400-900$ simulations each time, automatically varying the speed of the shepherd v_s and the number of agents N. This can be viewed in terms of a two-dimensional phase space corresponding to the scaled velocity $\frac{v_a}{v_s}$ of the agent (relative to the shepherd) and the scaled herd size $\frac{\sqrt{N}l_a}{l_s}$ (relative to that of an agent).

While the agent-based model provides a great illustration of the agent, herd, and optimal shepherd behavior under a variety of conditions, it does bring with it a reasonably high degree of complexity, even in minimal-model form. In order to extract the shapes that the herd takes on in response to a shepherd, it is valuable to examine the effective structure and dynamics of the herd via an ODE model corresponding to a minimal coarse-grained limit.

ODE model

In order to better understand how the herd–as a single entity that responds to a shepherd, we describe our system in the shepherd frame as a series of ordinary differential equations for the location, size and shape of the herd. Observations of herds in the real-world (Fig. 1) and in our ABM simulations (Fig. 2A, Movie S1) show that herd shapes can range from elliptical to lunate to ring-like. Thus, for the ODE model we need to represent the herd boundary using a parameterization that balances simplicity with the ability to take on the observed macroscopic shapes. As in the ABM model, the shepherd should have the ability to move toward/away or around the herd by varying the control parameters associated with its speed.

The herd's center is best described in the shepherd-centered frame by the polar variables R, θ, so that it is natural to describe the herd boundary also in polar coordinates as spanning both an angular width and a radial dimension, using a minimal parameterization to span the range of shapes from a narrow ring through a pinched lunate to an ellipse. If at one extreme, the herd assumes the shape of a uniform ring of thickness b while at the other it takes the form of a lunate shape of angular width $\frac{a}{R}$, the radial dimension of the herd can be written minimally as $r = R \pm b\sqrt{(1 - (\phi - \theta)^2/(a/R)^2)}$ i.e.

$$R^2 \frac{(\phi - \theta)^2}{a^2} + \frac{(r - R)^2}{b^2} = 1, \qquad (8)$$

which is the equation of an ellipse. where R and θ represent the position vector of the herd's center of mass with respect to the shepherd and θ is measured respect to a fixed x-axis (Fig. 1C). Here a represents the (polar) width of the herd and b represents the (radial) thickness of the herd (see 1C) we can write the area of the herd as $A = \pi ab$ (see SI *Herd boundary parameterization in our ODE framework*). The ratio of a and b specify the shape of the herd and can thus be conveniently captured by an aspect ratio $Q = \frac{a}{b}$. The form [8] accommodates shapes ranging from circular to ring-like as observed in simulations of the ABM model. In the limit $a/b \ll 1$, equation [8] describes a circular ring of radius R (Fig. 2B) and captures the shape of the herd in one of the herding phases observed in the ABM model (see Fig. 2A). When $a \sim b \sim R$, this equation describes a range of approximately elliptical and lunate shapes as seen in Fig. 2.

Having defined the variables of interest, we now consider the equations of motion for the location, size and shape of the herd in response to the shepherd using the following set of four ordinary differential equations (ODEs):

$$\ddot{R} = -\lambda_R(\dot{R} - u_R(t)) + f, \qquad (9)$$

$$\ddot{\theta} = -\lambda_\theta[\dot{\theta} - Q^{-1}u_\theta(t)], \qquad (10)$$

$$\dot{A} = -\lambda_A[A - A_0 - \gamma f + \zeta \frac{\bar{u_\theta}^2}{R}], \qquad (11)$$

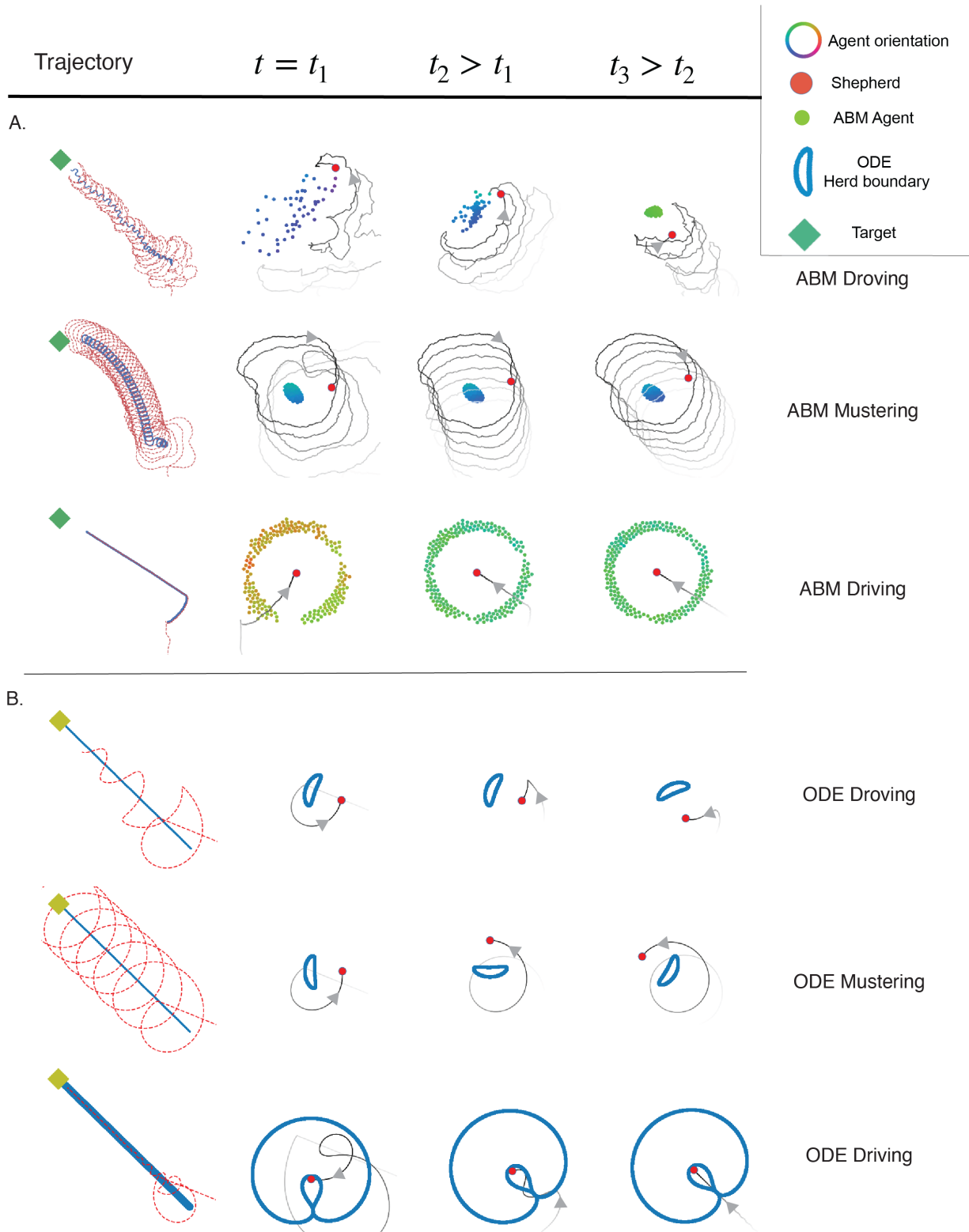$$\dot{Q} = -\lambda_Q[Q - Q_0 - \omega f]. \qquad (12)$$

FIG. 2: Shepherd and herd trajectories across three regimes in both the ABM and ODE models. Fig. 2A shows solutions to eqn. [1]. Trajectories correspond to movie S1 (see SI for exact parameter details). In each of the six plots in the left column, the mean path of the flock (blue) over an interval is shown as it is driven by a shepherd on a separate path (red) towards a target (green square). Columns 2-4 show snapshots from column 1, with trajectories indicated in black, where fading indicates history. From left to right, snapshots represent the flock at later timesteps. During droving (top row), a shepherd continuously collects the herd by panning left and right against the direction of movement while the herd slowly moves away from the shepherd and towards the target. During mustering (middle row), a shepherd prioritizes herd collection by cycling the herd repeatedly as it guides the herd towards the target. In driving (bottom row), the shepherd inserts itself inside the herd and relies on agent attraction to maintain herd cohesion while moving the herd towards the target. Fig. 2B shows solutions to equations [9-12]. Trajectories correspond to movie S2 (see SI for exact parameter details). Once again, snapshots show the flock boundary at three different times, with each row corresponding to the regimes in (A).

Here, $\lambda_{(.)}$ denote the time scales over which the herd responds to fluctuations in position, area or shape, ω and γ set the sensitivity of the herd's size and shape to the shepherd repulsion force, and ζ sets the sensitivity of the herd area to the rotational speed of the shepherd around the herd. The effect of the shepherd on the herd is characterized by f_0 which serves as the coefficient on a repulsive force with form $f = f_0 e^{-R/l_s}$, where l_s represents the characteristic length scale of shepherd repulsion. The shepherd can further affect the herd by changing its relative position by varying u_R and u_θ, the shepherd's radial and angular velocity respectively.

Equation [9] describes the movement of the herd towards or away from the shepherd (located at the origin). In the absence of a shepherd ($u_{R,\theta} = f_0 = 0$), the herd will either remain at rest if initialized at rest or eventually come to rest if initialized with some initial radial movement, $\dot{R} \neq 0$. With the addition of a shepherd the herd is repulsed with exponential decay as in the ABM model. If only repulsion were to exist, no control would be possible and the system would tend to equilibrium at $R \to \infty$. However, the shepherd can control the rate of herd escape by movement towards or away from the herd, leading to a net radial velocity of the herd that is the difference of the shepherd's motion and the herd's response, $\dot{R} - u_R$.

Equation [10] describes the orientation of the herd in response to the shepherd. In a manner similar to equation [9], the orientation of the herd tends to a constant equilibrium value of θ in the absence of control. The inclusion of u_θ in this equation simply states that the final rotation rate of the herd in the shepherd frame is the relative rate of rotation between the shepherd and the herd itself. The inverse aspect ratio Q^{-1} preceding u_θ in eqn. [10] denotes the increased sensitivity of the herd to shepherd rotation when it is in a more circular, symmetric, shape. When the herd is highly lunate in shape, rotation of the boundary of the herd is more difficult due to the lower symmetry of such a system. When we describe the 'rotation' of the herd, we refer to the change in orientation of the herd boundary in response to oscillatory, periodic, or steady movement of the shepherd.

Equation [11] describes the size of the herd in response to the shepherd. A_0 represents the equilibrium area of the herd, in the absence of a shepherd. As the shepherd draws nearer to the herd, increased pressure is put on the herd due to the f term and the herd changes size (in the ABM model, we notice that extreme values of f can lead to the herd splitting). The final term in eqn. [11] is based on observations from our ABM simulations. This term represents the compression of the herd associated with the shepherd circling around the herd, a behavior we explore in detail later in this paper ('mustering' is described at length in the section on *Three shepherding strategies*). Intuitively, the more rapidly the herd is encircled by the shepherd, the more compression of area

the herd experiences. In the final term, $\bar{u}_\theta$ represents the standard time-average and ensures that only consistent encircling of the herd (as opposed to sporadic and inconsistent) leads to compression. Finally, as one might expect intuitively, the effect of encircling the herd should decrease its area as the distance from the herd to the shepherd increases, which explains the $1/R$ factor in the final term of equation [11].

Equation [12] describes the aspect ratio of the herd (Fig. 1C), where Q_0 represents the relaxed aspect ratio of the herd and is chosen such that the herd, in the absence of the shepherd would take on an approximately circular shape. The herd's aspect ratio is affected by the shepherd's forcing term, f, which drives an increase in the aspect ratio and a correspond change in the herd shape from circular to lunate to ring-like (in the extreme).

Analogous to the ABM model described earlier, we then ask how can the shepherd control the herd's orientation, shape, and location. Since the ODE equations are formulated in the frame of the shepherd, there is no equivalent notion to the target distance as given in eqn. [7]. Thus, we formulate the following (similar) objective function:

$$W_{\text{angle}}|\theta - \theta_{\text{goal}}| + W_{\text{area}}A + W_R|R - nl_s| \qquad (13)$$

reflecting the shepherd's need to balance three goals: minimizing the angular deviation from the target direction θ_{goal}, minimizing the herd's area A, and minimizing the distance R between the shepherd and herd's CM.

Optimization the cost was carried out at each timestep by sampling u_R, u_θ in the range of $-u_R^{\max} \leq u_R(t) \leq u_R^{\max}$ and $-u_\theta^{\max} \leq, u_\theta(t) \leq u_\theta^{\max}$ (corresponding to moving towards the herd or around the herd) and chooses, at every timestep, the values of $u_R(t), u_\theta(t)$ that minimize the objective function (eqn. [13]). The values of W_{angle}, W_{area}, and W_R in eqn. [13] were chosen in analogy (but not in exact proportion) with those weights found in the ABM model with $\alpha >> W_{\text{area}} > W_R$ (see SI).

Due to the simpler nature of the ODE model, the ODE simulations were implemented using a home-brewed RK4 scheme in python, not C++, using the same discrete gradient descent approach for optimization described in the ABM model. Simulation plots were then created in two forms: the first form, shown in the right of all simulation videos (see Movie S2) represents the original ODE model from the shepherd-frame. The videos on the left show the entire ODE system placed onto a linear trajectory parallel to that observed in the ABM simulations to provide the reader a sense of what the lab-frame behavior of the herd-boundary looks like. While the lab-frame videos (Movie S2) provide an excellent depiction of the similarity between the ABM and ODE results, the exact trajectory and position of the target in the ODE lab-frame should not be interpreted literally.

Shepherding strategies

In every simulation in which the shepherd succeeds in guiding the herd to the target destination, the shepherd employs one of three distinct strategies or on occasion some combination thereof (Movie S1, S2).

Droving

In the first strategy, the shepherd sweeps back-and-forth orthogonal to the target direction to continuously collect and compress the herd as it moves forward. This "droving" strategy has been documented extensively in both nature [3] and prior simulations of shepherd interactions [15] (Top Rows of Fig. 2A-B, Fig. 4).

Mustering

In the second strategy, the shepherd continues its sweep all the way around the herd as it moves rather than in a back-and-forth motion, repeatedly encircling the herd. This strategy of "mustering" tends to occur when the herd is moving relatively quickly, as observed both in natural shepherding [23] and our simulations (Second Row of Fig. 2A-B, Fig. 4).

Driving

Finally, our simulations gave rise to a third unexpected strategy, in which the shepherd breaks into the herd (bottom rows of Fig. 2A-B, Fig. 4) and remains centrally within the herd, surrounded by the agents who do not come too close to the shepherd due to the repulsion between shepherd and agent.

Transitions between strategies

When the herd is relatively small, droving or mustering are the preferred strategy for flock transportation, with the choice of droving or mustering largely dependent on the scaled velocity of the shepherd. For faster shepherd velocities, droving emerges as the optimal solution as droving strikes the best balance between maintaining herd cohesion while encouraging a high rate of travel of the herd (due to the collecting and pushing elements of droving). As the scaled shepherd speed increases, there is a transition from droving to mustering. The shepherds' mustering motion emerges out of the constant desire to maintain herd cohesion while guiding the herd orientation. As the herd size gets larger, the relative speed at which mustering becomes dominant also decreases as bigger herds require even more of an emphasis on cohesion.

At large N, mustering is no longer feasible and the shepherd is seen to transition to driving. In all cases, when the speed of the agents are much faster than the agent and/or the herd size is sufficiently large, the system becomes uncontrollable.

Provided that herd coherence is strong enough to prevent fracturing to escape the central shepherd, the unique "driving" strategy allows the shepherd to drive and direct the herd directly towards the target. In this sense, driving is the most energy efficient strategy, but is available to the shepherd only when the risk of herd fragmentation is low. Driving is also seen to be the dominant control strategy when the inherent speed of the herd nearly matches that of the shepherd. At these speeds, when the herd is large, the shepherd does not have the time to either encircle the herd or collect and compress; then the shepherd must rely on the inherent herd attraction and alignment while using the driving strategy to affect overall herd orientation. This strategy persists even when the individual agent speed is faster than that of the shepherd (in contrast to droving and mustering) because of the circular shape of the herd formed during driving (Bottom Rows of Fig. 2A-B). However, the local herd density in this configuration is reduced, leading noise fluctuations to dominate the alignment and reduce the net velocity of the herd.

As discussed previously, the center of mass attraction of agents in the herd is essential for success of the driving strategy. To explore the nature of this dependence, we vary the value of γ in equation [1], which sets the weight of the center of mass attraction term. For each value of γ, we scanned the phase space and generated a corresponding phase diagram (see SI). We notice that reducing the attraction between agents significantly reduces the viability of the driving mode of transport, with driving entirely disappearing if the center of mass attraction is removed.

In the real world, shepherds may choose to optimize different elements of our objective function more than others. In order to understand the effect of how such a change would impact the phase diagram shown in Fig. 4, we vary the relative weight of W_{std} (see equation [7]) which determines the emphasis of the shepherd on herd cohesion (see SI) during the optimization process. We notice that reducing the focus on herd cohesion ($W_{std} \to 0.1W_{std}$) leads the driving phase to emerge at smaller herd sizes and leads to the disappearance of droving and mustering, leaving a surprising uncontrolled region in the phase diagram for small herd sizes. Because herds subjected to driving are inherently less dense, it is reasonable to expect that a reduction in the emphasis on herd cohesion would make driving more favorable. Similarly, the mustering and droving behaviors are a consequence of the shepherds' desire to maintain herd cohesion; when the impetus to maintain cohesion is lost, the mustering and droving phases also vanish. An implication of this result is that real shepherds in the wild must

be acutely aware of the size of the herd, for the droving and mustering behaviors observed in nature cannot be achieved in our model unless the cohesion weight in the objective function is relatively strong.

We also consider the effect of the agent size on the model behavior (see SI). Increasing the size of the agents in the herd leads to enlarged mustering and driving regimes and a reduction in the prevalence of droving. This is as expected, given that increasing the size of agents in the herd leads to less dense herds, and consequently results in less agent-agent alignment. When the herds are more diffuse and less aligned, the shepherd must work harder to maintain cohesion, leading to more mustering. Another way of understanding the increased prevalence in mustering and driving is to notice that increasing the size of agents in the herd has a similar effect to shifting the boundary of Fig. 4 to the right. In that scenario, mustering grows, droving reduces, and driving increases. Finally, we examine the impact of fixed herd sizes with varied agent sizes (see SI). For a fixed herd size, as N grows, we see an emergence of driving and a reduction of mustering.

We can categorize these behavioral modes in two ways, first by the behavior of the herd (as illustrated by Fig. 3) and second by the behavior of the shepherd (as illustrated in Fig. 4). We now consider the herd response independent of optimization and then explore the importance of our optimization from the perspective of the shepherd, as outlined by equation [7].

Minimal model of herd dynamics

Since all the behavioral modes are associated with an overall translation coupled to a global libration or oscillation, we plot the herd's angular velocity as a function of the herd orientation. In Fig. 3A), we show the periodic nature of the herd's response to the shepherd. Driving, in which the shepherd moves mostly linearly within the herd corresponds to a narrow cloud centered at the origin. In contrast, mustering and droving lead to analogs of oscillations and librations in $\psi - \dot{\psi}$ space (see SI: Classifying Shepherd Behavior in Frequency/Phase Space). Droving in ψ-$\dot{\psi}$ space form closed elliptical trajectories; as the the shepherd sweeps back and forth, the herd responds by shifting its orientation, analogous to a pendulum's oscillations about its equilibrium. Mustering, in contrast, is defined by a non-zero average angular velocity of the shepherd and that of the herd's average orientation (see Movie S1). As a result, mustering leads to the signature similar to that of a pendulum's libratory motion as shown in Fig 3. All these predicted behaviors are observed in our ABM simulations (Movie S1).

By extracting the experimental breathing rate from simulations (see SI) one can gather whether the predicted scaling of the herd's breathing rate captures the behav-
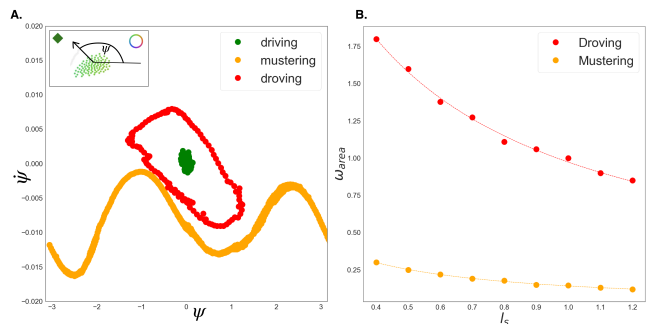

FIG. 3: Fig. 3A shows a description of each class of shepherding behavior (droving, driving, mustering) in ψ-$\dot{\psi}$ space, with data extracted steady-state periods of the ABM simulations (Movie S1). Droving: timesteps 400-600; Mustering: timesteps 6000-7000; Driving: timesteps 800-1000. Each ψ-$\dot{\psi}$ plot was scaled by the repulsion length-scale of the shepherd in that simulation and then shifted by the average angular orientation of the simulation (which is reasonable to do because the system is plotted in a periodic domain). Fig. 3B shows the relationship between shepherd length scale and frequency of the herd's area compression (breathing rate). Plot illustrates the calculated breathing rate of the circling or sweeping action in mustering and droving respectively along with the theoretical fit according to the predicted frequency $\omega = a \frac{v_s}{\sqrt{N}l_a + bl_s}$, where a and be represents constants corresponding to the shape of the shepherd's motion and its skew, accordingly. Dots represent breathing rates extracted using via the fourier representation and dashed lines represent fit. Fit params for droving are $a = 0.416, b = 0.328$. Fit params for mustering are $a = 0.046, b = 0.706$.

ior well. The results shown in Fig. 3B show that our prediction for the scaling rate is in fact quite a good representation of the herd's response to the shepherd in both the droving and mustering regimes.

Finally, we consider the phase-space of parameters corresponding to the scaled shepherd speed $(\frac{v_a}{v_s})$ and scaled herd size $(\frac{\sqrt{N}l_a}{l_s})$ in order to determine which shepherding strategy is optimal in each region of phase-space. Fig. 4 shows the optimal solution in phase space averaged over five scans of phase-space, each scan comprising between 400 and 900 simulations. Because the three shepherding strategies solve unique challenges, each is optimal in a different region of parameter space (Fig. 4). For a given interaction and optimal transport of the herd, we can observe all the three strategies by varying only two real-world parameters: the scaled herd size and scaled herd speed.

Herding efficiency

In addition to describing the shepherd behavior as an emergent solution to an optimal control problem, one can also describe the time-averaged steady-state behavior of the shepherding strategy via a parametric repre-
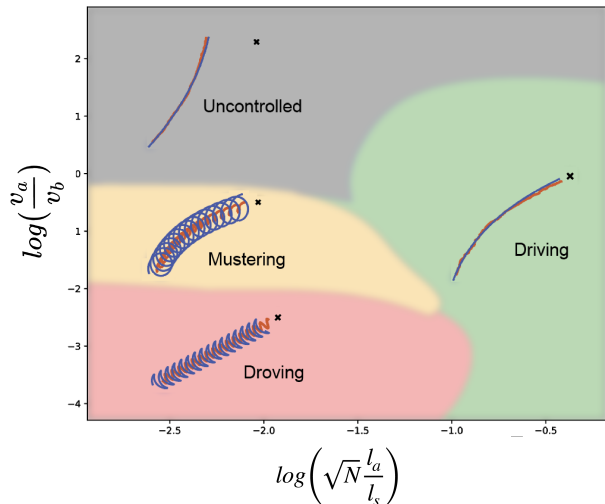
FIG. 4: Phase plot of herding regimes. For each combination of scaled swarm size (x-axis) and scaled swarm speed (y-axis), either the swarm could not be guided to the target with a single dog (gray), or it was most optimally guided with one of three herding strategy types: droving (red), mustering (orange), or driving (green). Overlayed on each regime is a sample agent-based trajectory of the center of mass of the herd (red line) and the center of mass of the shepherd (blue line), where the target location is represented by a black 'x.' The shaded background corresponds to best fit predictions for regime boundaries using SVM (SI methods), smoothed to reflect existence of overlap between regimes. Parameters are specified in SI tables (see SI)

.

sentation. Rotating our entire system (W.L.O.G.) such that the net velocity of the shepherd and herd towards the target, $\bar{v}_s$, is along the x-axis, we can describe the mean shepherd behavior by $x_s(t) = R_x cos(\omega t) + \bar{v}_s t$ and $y_s(t) = R_y sin(\omega t)$, where $\bar{v}_s$ is the mean translational speed of the shepherd, atop which there is a superposed oscillatory component with a frequency ω and amplitudes R_x and R_y along and perpendicular to the direction of motion.

In the droving regime, $R_x \sim 0, R_y \neq 0$ so that one has an oscillatory velocity component perpendicular to the direction of motion. In the mustering regime, $R_x \approx R_y \neq 0$ and the shepherd continuously circles around the herd leading to a low net drift speed $\bar{v}_s$. Finally, in the driving regime, $R_x \approx R_y \approx 0$. Observations of representative simulations (described in Movie S1) for different (scaled) herd sizes and (scaled) shepherd speed indicate that $\bar{v}_s^{droving} \sim \bar{v}_s^{driving} >> \bar{v}_s^{mustering}$ (see SI). Rescaling this drift speed by the number of agents we obtain a simple estimate of transport efficiency per agent that shows that driving is the most efficient means of transport, followed by droving, and then mustering. Although driving exhibits higher efficiency in steady-state it takes longer to reach steady-state. As expected, mustering trades off ef-

ficiency for herd compression. In all regimes a significant amount of time is spent initially gathering and orienting the herd. Finally, it is worth noting that, while higher effort strategies (such as mustering) may offer auxiliary benefits to including protection of a herd from an external threat or predator.

Discussion

Shepherding is a canonical example of the guided collective motion of social animals that exhibit swarm behavior, and is thus relevant to a number of phenomena such as livestock management, crowd control, environmental dynamics, and robotics.

Inspired by observations of herding across multiple species, here we have proposed and studied a minimal model of shepherding dynamics to explore the relationship between a herd, seeking to group together, and a shepherd, to optimally guide the herd towards a desired location. By investigating two complementary formulations of the underlying dynamics, we have distinguished three fundamentally distinct families of optimal shepherding behavior—mustering, droving, and driving—that emerge from our model in different parameter ranges (Fig. 2). While mustering and droving are commonly observed in natural settings, driving seems to be hitherto unreported regime wherein a shepherd guides a large and coherent herd from within and driving it with its own motion. Our phase diagram of herding regimes (Fig. 4) shows that each regime spans several orders of magnitude the scaled herd size $\sqrt{N}l_a/l_s$, and the scaled shepherd velocity v_a/v_s. Moving beyond the strategies to guide a herd to a target, we also considered the benefits and trade-offs in each strategy. A minimal model of efficiency measured by the time taken by the shepherd to transport a single agent show that droving is the most efficient way to transport small herds quickly while driving is most efficient for large cohesive herds.

While our analysis is a step towards understanding herding strategies, it also raises a number of questions. First, our minimal model ignores shepherd psychology, training, or biological motivations. Second, in relying on gradient-based optimization methods, our analysis cannot account for more involved, long-time-horizon shepherding strategies in which, for example, a shepherd sacrifices some degree of control to position itself or the herd for more optimal transport at a later time in the guiding process. Third, we leave unaddressed the scenario in which multiple shepherds can jointly guide a herd, where the potential for shepherd-shepherd coordination and task division might plausibly lead to additional families of optimal shepherding solutions. These are all natural questions for future study.

MATERIALS AND METHODS

Numerical integration of model equations

To simulate our ABM model formulation, we implemented a forward Euler timestepping algorithm to numerically integrate each system of model equations. The forward Euler was chosen because the ABM model describes a first-order system in which the velocity of the shepherd is directly chosen by the shepherd. As a result, a forward Euler approach most closely resembles the process of an agent making a decision, taking a step, and repeating the process. Additionally, the forward Euler approach was chosen for the ABM simulations in order because the first order system is not prone to numerical instability and so a first-order finite difference integration scheme is sufficient.

For the ODE model formulation, we implemented a standard RK4 integration method due to the presence of some second order terms in the ODE equations. Given that the ODE simulation time does not scale as N^2 and is rather constant for any number of agents (because we only solve for the system area) the RK4 scheme's improved stability is well worth the speed and simplicity tradeoff in this formulation.

Numerical optimization for model selection

The trajectory of the shepherd was optimized on a timestep by timestep basis, via a discrete gradient-descent style sampling for both the ABM simulations and ODE simulations. Parameter values are listed in Tables S1-3.

Code availability

Code will be made available for open access at https://github.com/arphysics/optimal-shepherding.

———————

[1] Tamás Vicsek, András Czirók, Eshel Ben-Jacob, Inon Cohen, and Ofer Shochet. Novel type of phase transition in a system of self-driven particles. Physical review letters, 75(6):1226, 1995.

[2] Iain D Couzin, Jens Krause, Richard James, Graeme D Ruxton, and Nigel R Franks. Collective memory and spatial sorting in animal groups. Journal of theoretical biology, 218(1):1–11, 2002.

[3] David JT Sumpter. Collective animal behavior. Princeton University Press, 2010.

[4] I Aoki. A simulation study on the schooling mechanism in fish. Bulletin of the Japanese Society of Fisheries, 48 (8):1081–1088, 1982.

[5] William H Warren and Daniel J Hannon. Direction of self-motion is perceived from optical flow. Nature, 336 (6195):162–163, 1988.

[6] William D Hamilton. Geometry for the selfish herd. Journal of theoretical Biology, 31(2):295–311, 1971.

[7] Andrew J King, Alan M Wilson, Simon D Wilshin, John Lowe, Hamed Haddadi, Stephen Hailes, and A Jennifer Morton. Selfish-herd behaviour of sheep under threat. Current Biology, 22(14):R561–R562, 2012.

[8] Craig W Reynolds. Flocks, herds and schools: A distributed behavioral model. In Proceedings of the 14th annual conference on Computer graphics and interactive techniques, pages 25–34, 1987.

[9] Andreas Huth and Christian Wissel. The simulation of the movement of fish schools. Journal of theoretical biology, 156(3):365–385, 1992.

[10] Ryan Lukeman, Yue-Xian Li, and Leah Edelstein-Keshet. Inferring individual rules from collective behavior. Proceedings of the National Academy of Sciences, 107(28):12576–12580, 2010.

[11] Jerome Buhl, David JT Sumpter, Iain D Couzin, Joe J Hale, Emma Despland, Edgar R Miller, and Steve J Simpson. From disorder to order in marching locusts. Science, 312(5778):1402–1406, 2006.

[12] Tamás Vicsek and Anna Zafeiris. Collective motion. Physics reports, 517(3-4):71–140, 2012.

[13] Alwyn Barry and Hugo Dalrymple-Smith. Visual communication and social structure–the group predation of lions. In Modelling Natural Action Selecton: Proceedings of an International Workshop, pages 146–151, 2005.

[14] Pushkin Kachroo, Samy A Shedied, John S Bay, and Hugh Vanlandingham. Dynamic programming solution for a class of pursuit evasion problems: the herding problem. IEEE Transactions on Systems, Man, and Cybernetics, Part C (Applications and Reviews), 31(1): 35–41, 2001.

[15] Daniel Strömbom, Richard P Mann, Alan M Wilson, Stephen Hailes, A Jennifer Morton, David JT Sumpter, and Andrew J King. Solving the shepherding problem: heuristics for herding autonomous, interacting agents. Journal of the royal society interface, 11(100):20140719, 2014.

[16] Brandon Bennett and Matthew Trafankowski. A comparative investigation of herding algorithms. In Proc. Symp. on Understanding and Modelling Collective Phenomena (UMoCoP), pages 33–38, 2012.

[17] Roger L Hughes. A continuum theory for the flow of pedestrians. Transportation Research Part B: Methodological, 36(6):507–535, 2002.

[18] Roger L Hughes. The flow of human crowds. Annual review of fluid mechanics, 35(1):169–182, 2003.

[19] Merv Fingas. The basics of oil spill cleanup. CRC press, 2012.

[20] Alan C Schultz and William Adams. Continuous localization using evidence grids. In Proceedings. 1998 IEEE International Conference on Robotics and Automation (Cat. No. 98CH36146), volume 4, pages 2833–2839. IEEE, 1998.

[21] Albert Froneman. Towards the management of bird

hazards on south african airports. Proceedings of the International Bird Strike Committee IBSC25/WP-SA5, Amsterdam, Netherlands, 2000.

[22] Ali E Turgut, Hande Çelikkanat, Fatih Gökçe, and Erol Şahin. Self-organized flocking in mobile robot swarms. Swarm Intelligence, 2(2):97–120, 2008.

[23] Lorna Coppinger, Raymond Coppinger, et al. Dogs for herding and guarding livestock. Livestock handling and transport, 13:235–253, 1993.